MR. CHUNCHUN LI (Orcid ID : 0000-0002-3657-5856)
PROFESSOR LIANG FANG (Orcid ID : 0000-0001-6568-3322)

Article type : Article

Low-firing and temperature stable microwave dielectric ceramics: $Ba_2LnV_3O_{11}$ (Ln = Nd, Sm)

Chunchun Li[1, 2*], Huaicheng Xiang[1], Minyu Xu[1], Jibran Khaliq[3], Junqi Chen[1], Liang Fang[1*]

[1]*State Key Laboratory Breeding Base of Nonferrous metals and specific Materials Processing, Guangxi universities key laboratory of non-ferrous metal oxide electronic functional materials and devices, College of Material Science and Engineering, Guilin University of Technology, Guilin, 541004, China*

[2]*College of Information Science and Engineering, Guilin University of Technology, Guilin, 541004, China*

[3]*Department of Mechanical and Construction Engineering, Faculty of Engineering and Environment, Northumbria University, Newcastle upon Tyne, NE1 8ST, United Kingdom*

Abstract

Low-firing and temperature stable microwave dielectric ceramics of $Ba_2LnV_3O_{11}$ (Ln = Nd, Sm) were prepared by solid-state reaction. X-ray diffraction (XRD) and scanning electron microscopy (SEM) were used to investigate the phase purity, crystal structure, sintering behavior, and microstructure. The XRD patterns indicated that $Ba_2LnV_3O_{11}$ (Ln =Nd, Sm) ceramics belong to monoclinic crystal system with $P2_1/c$ space group in the whole sintering temperature range (800-900 °C). Both ceramics could be well densified at 880 °C for 4 h with relative densities higher than 96%. The $Ba_2LnV_3O_{11}$ (Ln =Nd, Sm) samples

---

[*] Corresponding Author, fanglianggl001@aliyun.com; lichunchun2003@126.com

This article has been accepted for publication and undergone full peer review but has not been through the copyediting, typesetting, pagination and proofreading process, which may lead to differences between this version and the Version of Record. Please cite this article as doi: 10.1111/jace.15251

sintered at 880 °C for 4 h exhibited excellent microwave dielectric properties: ε_r = 12.05, $Q\times f$ = 23,010 GHz, τ_f = –7.7 ppm/°C, and ε_r = 12.19, $Q\times f$ = 27,120 GHz, τ_f = –16.2 ppm/°C, respectively. Besides, $Ba_2LnV_3O_{11}$ (Ln =Nd, Sm) ceramics could be well co-fired with the silver electrode at 880 °C.

Keywords: $Ba_2LnV_3O_{11}$ (Ln =Nd, Sm); Microwave dielectric properties; LTCC; Chemical compatibility.

1. Introduction

Microwave dielectric devices have been widely used in dielectric resonators, dielectric filters, and dielectric antennas, etc.[1, 2] In the last few decades, the rapid development in wireless communications, such as satellite broadcasting, radar transponder, 5G wireless systems, and Internet of Things (IoT), has led to extensive studies on the microwave dielectric ceramics with high performance.[3-6] For practical applications, an appropriate relative permittivity (ε_r), a near-zero temperature coefficient of resonant frequency (τ_f) for thermal stability, and a high quality factor ($Q\times f$) for frequency selectivity are crucially required.[7-10] In addition, in order to fulfill the rapidly increasing demand for miniaturization and integration, low temperature co-fired ceramic (LTCC) technology has gained substantial attention and vast development. LTCC technology has become a crucial step in the fabrication of integrated circuits. For LTCC applications, the microwave dielectric materials are primarily required to have low sintering temperatures to co-fire with the commonly used and highly conducting metals (e.g. 960 °C for Ag and 1083 °C for Cu).[11-14]

Recently, a large number of glass-free low temperature firing microwave dielectric materials have been reported. Most of them are based on the material systems with low-melting-points constituents, for example, $BiVO_4$,[15] $BaCaV_2O_7$,[16] $Ca_5Ni_4(VO_4)_6$,[17] Mg_2SiO_4.[18] In recent decades, good microwave dielectric properties have also been reported in some Ln-based vanadate ceramics.[19-21] For example, the $NdVO_4$ ceramic sintered at 1160 °C for 4 h possessed excellent microwave dielectric properties: ε_r = 12.0, $Q\times f$ = 36,440 GHz, and τ_f = –44.3 ppm/°C.[20] In our previous work, the microwave dielectric properties of compounds in the ternary vandates $BaO-Ln_2O_3-V_2O_5$ were characterized. Among them, $Ba_2LaV_3O_{11}$ has attracted extensive attention in recent years due to its excellent microwave dielectric properties (ε_r = 12.8, $Q\times f$ = 31,800 GHz, and τ_f = –14.0 ppm/°C), and low sintering temperature (840 °C).[22] We also found that $Ba_2BiV_3O_{11}$ ceramic could be densified at 870 °C and possessed good microwave dielectric properties with ε_r = 14.2, $Q\times f$ = 68,700 GHz, and τ_f = –81.0 ppm/°C.[23] This stimulates us to investigate whether other compounds in $Ba_2LnV_3O_{11}$ system exhibit good microwave dielectric properties. Therefore, in this work, $Ba_2LnV_3O_{11}$ (Ln = Nd, Sm) ceramics were prepared with an attempt to develop novel low-firing ceramics. The microstructures and microwave dielectric properties were investigated. Their chemical compatibility with silver (Ag) has also been investigated.

2. Experimental section

2.1. Preparation

$Ba_2LnV_3O_{11}$ ceramics were prepared by the conventional solid state method with high-purity $BaCO_3$, Nd_2O_3, Sm_2O_3, and NH_4VO_3 (> 99%, Guo-Yao Co., Ltd., Shanghai, China) as starting reagents. The stoichiometrically weighed powders were mixed and ball-milled in alcohol medium for 6 h, followed by drying at 120 ^{o}C. The dried powers were calcined at 750 ^{o}C for 4 h, and then re-milled for 6 h. The resultant powders were granulated with polyvinyl alcohol (PVA, 10 vol%) as a binder, and pressed into cylindrical pellets of 10 mm in diameter and 6 mm in thickness in a steel die under a pressure of 350 MPa. The pellets were first heated at 550 ^{o}C in air for 4 h at a heating rate of 1.5 ^{o}C/min to burn out the organic binder, and then sintered over a temperature range of 800 ^{o}C–900 ^{o}C for 4 h with a heating rate of 5 ^{o}C/min.

2.2 Characterizations

The powder X-ray diffraction (XRD) (Cu$K\alpha 1$, 1.54059 Å, Model X'Pert PRO, PANalytical, Almelo, Holland) was carried out on the calcined powders to identify the crystal structure and phase purity. The microstructures of the ceramics were characterized by field emission scanning electron microscopy (FE-SEM, Model S4800, Hitachi, Japan). The densities of the sintered ceramics were determined using the Archimedes' method. The dielectric properties at microwave frequencies were recorded by the network analyzer (Model N5230A, Agilent Co., Palo Alto, California) and temperature chamber (Delta 9039, Delta Design, San Diego, CA). The temperature coefficient of resonant frequency (τ_f) was calculated by the equation:

$$\tau_f = \frac{f_{T_1} - f_{T_0}}{f_{T_0}(T_1 - T_0)} \quad (1)$$

where, f_{T_1} and f_{T_0} were the resonant frequencies at 85 °C and room temperature, respectively.

3. Results and discussion

3.1 Structure and morphology

Fig. 1(a) depicts the XRD patterns of the calcined $Ba_2NdV_3O_{11}$ and $Ba_2SmV_3O_{11}$ powders at 750 °C for 4 h. Both compounds exhibited similar diffraction patterns and all the observed peaks matched well with the standard card JCPDS No. 40-0105 for $Ba_2LaV_3O_{11}$. This result indicates that $Ba_2NdV_3O_{11}$ and $Ba_2SmV_3O_{11}$ well crystallized in single phase with a monoclinic space group $P2_1/c$ (14). The lattice parameters were calculated by the least square refinement with a = 12.37 Å, b = 7.76 Å, c = 11.26 Å, β = 103.5°, and V = 1051.82 $Å^3$ for $Ba_2NdV_3O_{11}$ and a = 12.35 Å, b = 7.74 Å, c = 11.23 Å, β = 103.2 °, and V = 1047.12 $Å^3$ for $Ba_2SmV_3O_{11}$, respectively. The schematic of crystal structure for $Ba_2LnV_3O_{11}$ is shown in Fig. 1(b). As shown, Ln atoms are six-coordinated in distorted octahedra and $[LnO_6]$ octahedra are edge-sharing, while V atoms are connected with four neighboring oxygen forming $[VO_4]$ tetrahedra. The adjacent $[LnO_6]$ octahedra and $[VO_4]$ tetrahedra are corner shared. Ba atoms are located in the interspace of the tetrahedra and octahedra.

Fig. 2(a-e) shows SEM micrographs of $Ba_2NdV_3O_{11}$ ceramics sintered at 820 °C to 900 °C and Fig. 2(f) for $Ba_2SmV_3O_{11}$ sintered at 880 °C. As shown, a porous microstructure with an average grain size of 1–2 μm was observed in the $Ba_2NdV_3O_{11}$ samples sintered at 820 °C. With the increasing sintering temperature, the amount of pore decreased and the grains gradually grew up. As the sintering temperature increased to 880 ^{o}C, a homogeneous microstructure with evidently identifiable grain boundaries was obtained for $Ba_2NdV_3O_{11}$. However, further increase in sintering temperature to 900 ^{o}C induced abnormal grain growth with large grains (~ 6 μm). Similar phenomena were observed in $Ba_2SmV_3O_{11}$ ceramics, and the ceramic sintered at 880 ^{o}C exhibited dense microstructure with closely-packed grains, as shown in Fig. 2(f).

3.2 Microwave dielectric properties

The variations in the relative density and relative permittivity of the $Ba_2LnV_3O_{11}$ ceramics as a function of sintering temperature are shown in Fig. 3. With increasing sintering temperature, the relative density gradually increased to a maximum value and then declined slightly. The optimum densification temperatures for both ceramics were determined to be 880 ^{o}C with a maximum relative density of 96.2 % for $Ba_2NdV_3O_{11}$ and 97.1 % for $Ba_2SmV_3O_{11}$ ceramic, respectively.

As shown in Fig. 3(b), the relative permittivity (ε_r) exhibited a similar variation trend with the increasing sintering temperature to the density and the saturated ε_r values were achieved in the best sintered samples with ε_r = 12.05 for $Ba_2NdV_3O_{11}$ and 12.19 for $Ba_2SmV_3O_{11}$, respectively. This result suggests the crucial effect of density on the relative permittivity, especially for the samples with porosity. Thus, to eliminate the effects of porosity, the relative permittivity was corrected according to by the Bosman and Having's porosity correction equation:[24, 25]

$$\varepsilon_{corr} = \varepsilon_r (1 + 1.5p) \qquad (2)$$

where, p is the fractional porosity. The ε_{corr} values of $Ba_2LnV_3O_{11}$ (Ln = Nd, Sm) ceramics at 880 °C are about 12.73 and 12.74, respectively. Besides, the theoretical permittivity was evaluated according to Clausius–Mossotti equation:[26, 27]

$$\varepsilon_r = \frac{1+2b\alpha_D^T/V_m}{1-b\alpha_D^T/V_m} \tag{3}$$

where, $b = 4\pi/3$, α_D^T is the molecular polarizability and V_m is the cell volume. The calculated theoretical permittivity of $Ba_2NdV_3O_{11}$ is 12.14 and 12.09 for $Ba_2SmV_3O_{11}$. The slightly higher theoretical permittivity of $Ba_2NdV_3O_{11}$ than its Sm counterpart could be due to the larger ionic polarizability of Nd^{3+} (5.01 Å) than Sm^{3+} (4.74 Å). Additionally, the relative error between the porosity corrected ε_r and the theoretical density is about 7.2% for the $Ba_2NdV_3O_{11}$ ceramic and 8.3% for $Ba_2SmV_3O_{11}$ ceramic, which indicates that ionic polarization plays a prominent role in the dielectric polarizability in the microwave frequency region.[11, 28]

Fig. 4 shows the $Q\times f$ and τ_f values of the $Ba_2NdV_3O_{11}$ and $Ba_2SmV_3O_{11}$ ceramics sintered at different temperatures for 4 h. Similar to the density and relative permittivity, the quality factors also exhibited strong dependency on the sintering temperature. With increasing sintering temperature, the $Q\times f$ values initially increased to a maximum value and then decreased. The maximum $Q\times f$ values of 23,010 GHz for $Ba_2NdV_3O_{11}$ and 27,120 GHz for $Ba_2SmV_3O_{11}$ were obtained at 880 °C for 4 h, respectively. In general, the $Q\times f$ value depends on the intrinsic parameters such as structural characteristics and the extrinsic parameters such as porosity, secondary phases, and lattice defects.[29, 30] For ceramics with high relative densities > 95 % and no secondary phases, the extrinsic impacts on $Q\times f$ value could be depressed. According to the study of Kim *et al.*,[31] the $Q\times f$ also could be highly dependent on the packing fraction. The packing fraction could be calculated by the equation:

$$packing\,fraction\,(\%) = \frac{volume\,of\;\,packed\,ions}{volume\,of\;\,unit\,cell} \times Z \tag{4}$$

where, Z is the number of formula units per unit cell. The packing fraction of $Ba_2NdV_3O_{11}$ is 57.9 %, and 58.1 % for $Ba_2SmV_3O_{11}$. For comparison, the calculated packing fractions for $Ba_2LnV_3O_{11}$ (Ln = Bi, La, Nd, Sm) ceramics are listed in Table 1. $Ba_2LnV_3O_{11}$ ceramics with lower Ln-site ionic radius decreased the unit cell volume, which in turn increased the packing fraction. It is obviously seen that a larger packing fraction directly corresponds to a higher $Q\times f$ value. Therefore, the variation in the $Q\times f$ value of $Ba_2LnV_3O_{11}$ (Ln = Bi, La, Nd, Sm) ceramics could be explained by the difference in packing faction.[32] The increase in packing fraction indicates that the space for lattice vibrations decreases, and thus reduces the intrinsic loss.

As presented in Fig. 4(b), over the sintering temperature range from 800-900 ^{o}C, no significant change in the τ_f value was observed. When sintered at 880 ^{o}C for 4 h, $Ba_2NdV_3O_{11}$ possessed a near-zero τ_f value of –7.7 ppm/^{o}C while $Ba_2SmV_3O_{11}$ had a relatively negative τ_f value of –16.2 ppm/^{o}C. The τ_f value is a function of the temperature coefficient of the dielectric constant (τ_ε) and the linear thermal expansion coefficient (α_L), as show in equation:[33]

$$\tau_f = -(\frac{\tau_\varepsilon}{2} + \alpha_L) \tag{5}$$

where, α_L is a typically constant for dielectric ceramics, and τ_ε depends on the tilting of oxygen octahedral.[34] The degree of tilting on oxygen octahedral could be reflected by the bond valence and bond length between the cations and oxygen atoms. According to the bond valence theory, the τ_f value is related to chemical nature of ions, the distance between cations and anions, the bond valence of oxygen octahedra.[35, 36]

According to Fig. 1(b), Ln atoms are six-coordinated in octahedra. The bond valences between Ln cations and oxygen ions of the $Ba_2LnV_3O_{11}$ ceramics calculated by the following formulas:

$$V_\mathrm{i} = \sum_j v_{ij} \tag{6}$$

$$v_\mathrm{ij} = \exp\left[\frac{R_{ij} - d_{ij}}{b}\right] \tag{7}$$

where R_ij is the bond valence parameter, d_ij is the length of a bond between atoms i and j, and b is a universal constant (0.37 Å).[37] As shown in Table 1, V_{Ln} is 3.082 and 3.305 for $Ba_2NdV_3O_{11}$ and $Ba_2SmV_3O_{11}$. The increase in bond valence of Ln cation results in an increase in bond strength between Ln cation with oxygen, which in turn increases the thermal energy for tilted structure recovering, and thus τ_f value decreased.[38]

3.3 Chemical compatibility with silver electrode

For LTCC applications, the microwave dielectric materials should have chemical compatibility with metal electrodes. Silver is a commonly used electrode material because of its high electric conductivity and relatively low price. In the present work, 15 wt% Ag powder was mixed with the $Ba_2LnV_3O_{11}$ (Ln = Nd, Sm) and co-fired at 880 $^\mathrm{o}$C for 4 h to confirm their chemical compatibility. XRD patterns and SEM images of the co-fired ceramics are shown in Fig. 5. Only the diffraction peaks of $Ba_2LnV_3O_{11}$ (Ln = Nd, Sm) and silver (marked with “Ag” in Fig.5) were detected in the XRD patterns. Additionally, SEM images showed two different kinds of grains with the larger grains to be Ag. Thus, no chemical reaction occurred between the $Ba_2LnV_3O_{11}$ (Ln = Nd, Sm) ceramics and Ag electrode when sintered at 880 ^{o}C for 4 h. All the results indicate that $Ba_2LnV_3O_{11}$ (Ln = Nd, Sm) ceramics could be possible candidates for applications in LTCC technology due to their low sintering temperature, excellent microwave dielectric properties, and reliable compatibility with silver electrodes.

Table 2 displays the sintering temperatures, microwave dielectric properties and chemical compatibility with Ag electrode of some LTCC materials. All these ceramics possess low sintering temperatures (lower than 960 ^{o}C) except for $NdVO_4$. The microwave permittivity of the $Ba_2LnV_3O_{11}$ (Ln = Nd, Sm) ceramics is comparable to the garnet structured $Na_2LnMg_2V_3O_{12}$ (Ln = Nd, Sm), whereas the quality factor is inferior to $BaMg_2(VO_4)_2$. However, $Ba_2LnV_3O_{11}$ (Ln = Nd, Sm) ceramics possess near-zero τ_f values, which guarantees the thermal stability of materials and devices.

3.4 Thermal expansion

The variable-temperature (VT) XRD patterns performed on $Ba_2LnV_3O_{11}$ (Ln = Nd, Sm) over 25-120 ^{o}C are shown in Fig. 6. It is obvious that the main peaks of both ceramics slightly shifted with increasing measurement temperature, indicating the variation in the lattice parameters and cell volume. The unit cell parameters of $Ba_2LnV_3O_{11}$ (Ln = Nd, Sm) ceramics were refined using the least square method and shown in Fig. 7 as a function of temperature from 25 to 120 ^{o}C. As the temperature increased, the cell parameters a, b, c, and V slightly increased for both ceramics. This indicates $Ba_2LnV_3O_{11}$ (Ln = Nd, Sm) ceramics have positive thermal expansion coefficient. From 25 to 120 ^{o}C, the thermal expansion coefficient coefficients of $\alpha_a = 1.47\times10^{-6}$ and 1.73×10^{-6} K^{-1}, $\alpha_b = 2.80\times10^{-6}$ and 3.15×10^{-6} K^{-1}, $\alpha_c = 2.14\times10^{-6}$ and 2.08×10^{-6} K^{-1}, $\alpha_V = 2.36\times10^{-6}$ and 2.65×10^{-6} K^{-1} for $Ba_2LnV_3O_{11}$ and $Ba_2LnV_3O_{11}$, respectively.

4. Conclusions

This work has shown that low temperature sintering process could able to prepare the $Ba_2LnV_3O_{11}$ (Ln =Nd, Sm) single phase. The X-ray diffraction analyses indicated that $Ba_2LnV_3O_{11}$ (Ln =Nd, Sm) ceramics belong to monoclinic system with $P2_1/c$ space group in the whole sintering temperature range. $Ba_2LnV_3O_{11}$ (Ln =Nd, Sm) ceramics could be well densified at temperature at 880 °C with relative densities higher than 96%. The $Ba_2LnV_3O_{11}$ (Ln =Nd, Sm) samples sintered at 880 °C for 4 h exhibited excellent microwave dielectric properties: ε_r = 12.05 and 12.19, $Q\times f$ = 23,010 GHz and 27,120 GHz, τ_f = –7.7 ppm/°C and –16.2 ppm/°C, respectively. Additionally, $Ba_2LnV_3O_{11}$ (Ln =Nd, Sm) ceramics could be co-fired with the silver electrode at 880 °C. All the results indicate that the $Ba_2LnV_3O_{11}$ (Ln =Nd, Sm) ceramics are suitable materials in LTCC applications.

Acknowledgments

This work was supported by Natural Science Foundation of China (Nos. 21561008, 51502047, and 21761008), the Natural Science Foundation of Guangxi Zhuang Autonomous Region (Nos. 2015GXNSFFA139003, 2016GXNSFBA380134, and 2016GXNSFAA380018), Project of Scientific Research and Technical Exploitation Program of Guilin (2016010702-2), Innovation Project of Guangxi Graduate Education (YCBZ2017052), and the Project of Department of Science and Technology of Guangxi (2015AA07036). We appreciate for Collaborative Innovation Center for Exploration of Hidden Nonferrous Metal Deposits and Development of New Materials in Guangxi for the financial support.

References

1.Cava RJ. Dielectric materials for applications in microwave communications. *J Mater Chem*. 2001;11:54–62.

2. Fujii T, Ando A, Sakabe Y. Charaterization of dielectric properties of oxide materials in frequency range from GHz to THz. *J Eur Ceram Soc*. 2006;26:1857–1860.

3. Zhou D, Pang LX, Wang H, Yao X. Low temperature firing microwave dielectric ceramics $(K_{0.5}Ln_{0.5})MoO_4$ (Ln = Nd and Sm) with low dielectric loss. *J Eur Ceram Soc*. 2011;31:2749–52.

4. Reaney IM, Iddles D. Mcrowave dielectric ceramics for resonators and filters in mobile phone networks. *J Am Ceram Soc*. 2006;89:2063–72.

5. Valant M, Suvorov D. Glass-free low-temperature cofired ceramics: calcium germanates, silicates and tellurates. *J Eur Ceram Soc*. 2004;24:1715–9.

6. Xiang HC, Fang L, Fang WS, Tang Y, Li CC. A novel low-firing microwave dielectric ceramic $Li_2ZnGe_3O_8$ with cubic spinel structure. *J Eur Ceram Soc*. 2017;37:625–629.

7. Hu CZ, Fang L, Su HP, Liu LJ, Wu BL. Effects of Sr substitution on microwave dielectric properties of $Ba_3LaNb_3O_{12}$ ceramics. *J Alloys Compd*. 2009;487:504–506.

8. Wakino K. Miniaturization techniques of microwave components for mobile communications systems—using low loss dielectrics. *Ferroelectr Rev*. 2000;22:1–49.

9. Lei W, Lu WZ, Liu D, Zhu JH. Phase evolution and microwave dielectric properties of $(1\text{-}x)ZnAl_2O_4\text{-}xMg_2TiO_4$ ceramics. *J Am Ceram Soc*. 2009;92:105–109.

10. Zhou D, Guo D, Li WB, Pang LX, Yao X, Wang DW, Reaney IM. Novel temperature stable high-er microwave dielectrics in the Bi_2O_3–TiO_2–V_2O_5 system. *J Mater Chem C.*

2016;4:5357–5362.

11. Zhou D, Randall CA, Wang H, Yao X. Microwave dielectric properties of Li_2WO_4 ceramic with ultra-low sintering temperature. *J Am Ceram Soc*. 2011;94:348–350.

12. Lei W, Lu WZ, Zhu JH, Wang XH. Microwave dielectric properties of $ZnAl_2O_4$-TiO_2 spinel-based composites. *Mater Lett*. 2007;61:4066–4069.

13. Takada T, Wang SF, Yoshikawa S, Jang SJ, Newnham RE. Effect of glassadditions on $BaO–TiO_2–WO_3$ microwave ceramics. *J Am Ceram Soc.* 1994;77:1909–16.

14. Fang L, Su CX, Zhou HF, Wei ZH, Zhang H. Novel low-firing microwave dielectric ceramic $LiCa_3MgV_3O_{12}$ with low dielectric loss. *J Am Ceram Soc*. 2013;96:688–690.

15. Pang LX, Zhou D, Qi ZM, Liu WG, Yue ZX, Reaney IM. Structure–property relationships of low sintering temperature scheelite-structured $(1-x)BiVO_4–xLaNbO_4$ microwave dielectric ceramics. *J Mater Chem C.* 2017;5:2695–2701.

16. Jiang XW, Li CC, Su CX, Wei ZH, Fang L. Low temperature firing and microwave dielectric properties of $BaCaV_2O_7$ ceramics. *Ceram Int*. 2015;41:5172–5176.

17. Wang D, Xiang HC, Tang Y, Fang L, Khaliq J, Li CC, A low-firing $Ca_5Ni_4(VO_4)_6$ ceramic with tunable microwave dielectric properties and chemical compatibility with Ag. *Ceram Int*. 2016:42;15094–15098.

18. Zhang J, Yue ZX, Luo Y, Zhang XH, Li LT, Novel low-firing forsterite-based microwave dielectric for LTCC applications. *J Am Ceram Soc*. 2016;99:1122–1124.

19. Wang Y, Zuo RZ, Zhang C, Zhang J, Zhang TW, Low-temperature-fired $ReVO_4$ (Re=La, Ce) microwave dielectric ceramics. *J Am Ceram Soc*. 2015;98:1–4.

20. Li W, Fang L, Sun YH, Tang Y, Chen JW, Li CC, Preparation, crystal structure and

microwave dielectric properties of rare-earth vanadates: $ReVO_4$ (Re = Nd, Sm). *J Electron Mater*. 2017;46:1956–1962.

21. Tang Y, Jiang XW, Xiang HC, Li CC, Fang L, Xing XR. Two novel low-firing $Na_2AMg_2V_3O_{12}$ (A = Nd, Sm) ceramics and their chemical compatibility with silver. *Ceram Int*. 2017;43:2892–2898.
22. Li J, Fang L, Luo H, Tang Y, Li CC. Structure and microwave dielectric properties of a novel temperature stable low-firing $Ba_2LaV_3O_{11}$ ceramic. *J Eur Ceram Soc*. 2016;36:2143–2148.
23. Li J, Li CC, Wei ZH, Tang Y, Su CX, Fang L. Microwave dielectric properties of a low-firing $Ba_2BiV_3O_{11}$ ceramic. *J Am Ceram Soc*. 2015;98:683–686.
24. Penn SJ, Alford NM, Templeton A, Wang XR, Xu MS, Reece M, Schrapel K. Effect of porosity and grain size on the microwave dielectric properties of sintered alumina. *J Am Ceram Soc*. 1997;80:1885–8.
25. Bosman AJ, Havinga EE. Temperature dependence of dielectric constants of cubic ionic compounds. *Phys Rev*. 1963;129:1593–600.
26. Shannon RD. Dielectric polarizabilities of ions in oxides and fluorides. *J Appl Phys*. 1993;73:348–366.
27. Yoon SH, Kim DW, Cho SY, Sun HK. Investigation of the relations between structure and microwave dielectric properties of divalent metal tungstate compounds. *J Eur Ceram Soc*. 2006;26:2051–2054.
28. Li J, Fang L, Luo H, Khaliq J, Tang Y, Li CC. Li_4WO_5: A temperature stable low-firing microwave dielectric ceramic with rock salt structure. *J Eur Ceram Soc*.

2016;36:243–246.

29. Zhou D, Randall CA, Baker A, Wang H, Pang LX, Yao X. Dielectric properties of an ultra-low-temperature cofiring $Bi_2Mo_2O_9$ multilayer. *J Am Ceram Soc*. 2010;93:1443–1446.

30. Chen YC, Wang YN, Hsu CH. Enhancement microwave dielectric properties of Mg_2SnO_4 ceramics by substituting Mg^{2+} with Ni^{2+}. *Mater Chem Phys*. 2012;133:829–33.

31. Kim ES, Chun BS, Freer R, Cernik RJ. Effects of packing fraction and bond valence on microwave dielectric properties of $A^{2+}B^{6+}O_4$ (A^{2+}: Ca, Pb, Ba; B^{6+}: Mo, W) ceramics. *J Eur Ceram Soc*. 2010;30:1731–1736.

32. Galasso FS, Kurti N, Smoluchowski R. *Structure and properties of inorganic solids*. Pergamon Press, 1970.

33. Reaney IM, Colla EL, Setter N. Dielectric and structural characteristics of Ba- and Sr-based complex perovskites as a function of tolerance factor. *Jpn Appl Phys*. 1994;33:984–3990.

34. Hirata T. Oxygen position, octahedral distortion, and bond-valence parameter from bond lengths in $Ti_{1-x}Sn_xO2$, ($0 \leq x \leq 1$). *J Am Ceram Soc*. 2000;83:3205–3207.

35. Kim WS, Yoon KH. Microwave dielectric properties and far-infrared reflectivity characteristics of the $CaTiO_3$–$Li_{(1/2)-3x}Sm_{(1/2)+x}TiO_3$ ceramics. *J Am Ceram Soc*. 2000;83:2327–29.

36. Zhou D, Wang H, Pang LXi, Randall CA, Yao X. $Bi2O_3$–MoO_3 Binary system: an alternative ultralow sintering temperature microwave dielectric. *J Am Ceram Soc*. 2009;92:2242–2246.

37. Brese NE, O'Keeffe M. Bond-valence parameters for solids. *Acta Crystallogr*. 1991;B47:192–197.

38. Moulson AJ, Herbert JM. *Electroceramics: materials, properties, applications*. Wiley, 2003.

39. Fang L, Guo HH, Fang WS, Wei ZH, Li CC. $BaTa_2V_2O_{11}$: A novel low fired microwave dielectric ceramic. *J Eur Ceram Soc*. 2015;35:3765–3770.

40. Joung M R, Kim JS, Song ME, Nahm S, Paik JH. Formation process and microwave dielectric properties of the $R_2V_2O_7$ (R=Ba, Sr and Ca) Ceramics. *J. Am. Ceram. Soc*. 2009;92:3092–3094.

41. Wang Y, Zuo RZ. A novel low-temperature fired microwave dielectric ceramic $BaMg_2V_2O_8$ with ultra-low loss. *J Eur Ceram Soc*. 2016;36:247–251.

42. Suresh EK, Prasad K, Arun NS, Ratheesh R. Synthesis and microwave dielectric properties of $A_{16}V_{18}V_{61}$ (A = Ba, Sr and Ca) ceramics for LTCC applications. *J Electron Mater*. 2016;45:2996–3002.

43. Tang Y, Jiang XW, Xiang HC, Li CC, Fang L, Xing XR. Two novel low-firing $Na_2AMg_2V_3O_{12}$(A=Nd, Sm) ceramics and their chemical compatibility with silver. *Ceram Int*. 2017;43;2892–2898.

Table 1 The packing fraction, bond valence and microwave dielectric properties of $Ba_2LnV_3O_{11}$ (Ln = Bi, La, Nd, and Sm) ceramics

Ceramics	S.T. (°C)	ε_r	$Q\times f$ (GHz)	τ_f (ppm/°C)	Unit cell Volume(Å^3)	Packing fraction (%)	$V_{Ln\text{–}O}$	Reference
$Ba_2BiV_3O_{11}$	870	14.20	68,700	–81	1049.40	59.5	3.081	[23]
$Ba_2LaV_3O_{11}$	840	12.80	31,800	–14	1066.80	58.5	3.481	[22]
$Ba_2NdV_3O_{11}$	880	12.05	23,010	–7.7	1051.82	57.9	3.082	This work
$Ba_2SmV_3O_{11}$	880	12.19	27,120	–16.2	1047.12	58.1	3.305	This work

Table 2 Sintering temperatures, microwave dielectric properties and chemical compatibility with Ag of some LTCC ceramics

Ceramics	S.T. (^{o}C)	ε_r	$Q\times f$ (GHz)	τ_f (ppm/^{o}C)	Reactivity with Ag	Reference
$Ba_2NdV_3O_{11}$	880	12.05	23,010	–7.7	No	This work
$Ba_2SmV_3O_{11}$	880	12.19	27,120	–16.2	No	This work
$Ba_2V_2O_7$	900	10.1	51,630	–26.5	No report	[40]
$BaCaV_2O_7$	830	8.9	31,362	–68.2	No report	[16]
$BaTa_2V_2O_{11}$	870	28.2	41,958	+90	Yes	[39]
$BaMg_2(VO_4)_2$	900	12	156,140	–36	No report	[41]
$Ba_{16}V_{18}O_{61}$	620	9.7	80,100	–61	No	[42]
$NdVO_4$	1160	12	36,440	–44.3	No report	[20]
$Na_2NdMg_2V_3O_{12}$	850	12	26,544	–63	No	[43]
$Na_2SmMg_2V_3O_{12}$	850	12.1	36,207	–69	No	[43]

Figure Captions:

Fig.1 The standard $Ba_2LaV_3O_{11}$ (No. 40-0105) profile as well as the XRD patterns of the calcined $Ba_2NdV_3O_{11}$ and $Ba_2SmV_3O_{11}$ (a), and the schematic crystal structure of $Ba_2LnV_3O_{11}$ (Ln = Nd, Sm) (b).

Fig.2 SEM micrographs of $Ba_2NdV_3O_{11}$ ceramics sintered at 820 ^{o}C to 900 ^{o}C (a-e) and $Ba_2SmV_3O_{11}$ sintered at 880 ^{o}C (f).

Fig.3 Variation in relative density (a) and relative permittivity (b) of the $Ba_2NdV_3O_{11}$ and $Ba_2SmV_3O_{11}$ ceramics as a function of sintering temperature.

Fig.4 $Q\times f$ and τ_f values of the $Ba_2NdV_3O_{11}$ and $Ba_2SmV_3O_{11}$ ceramics sintered at different temperatures for 4 h (the loss tangent shown in the inset).

Fig.5 The XRD patterns and backscattered electron (BSE) images of $Ba_2LnV_3O_{11}$ (Ln = Nd, Sm) ceramics with 15 wt% Ag cofired at 880 ^{o}C.

Fig.6 Selected VT-XRD patterens of $Ba_2LnV_3O_{11}$ (Ln = Nd, Sm) ceramics over 25-120 ^{o}C.

Fig.7 The variation in unit cell parameters (a, b, c, and V) of $Ba_2LnV_3O_{11}$ (Ln = Nd, Sm) over 25-120 ^{o}C.

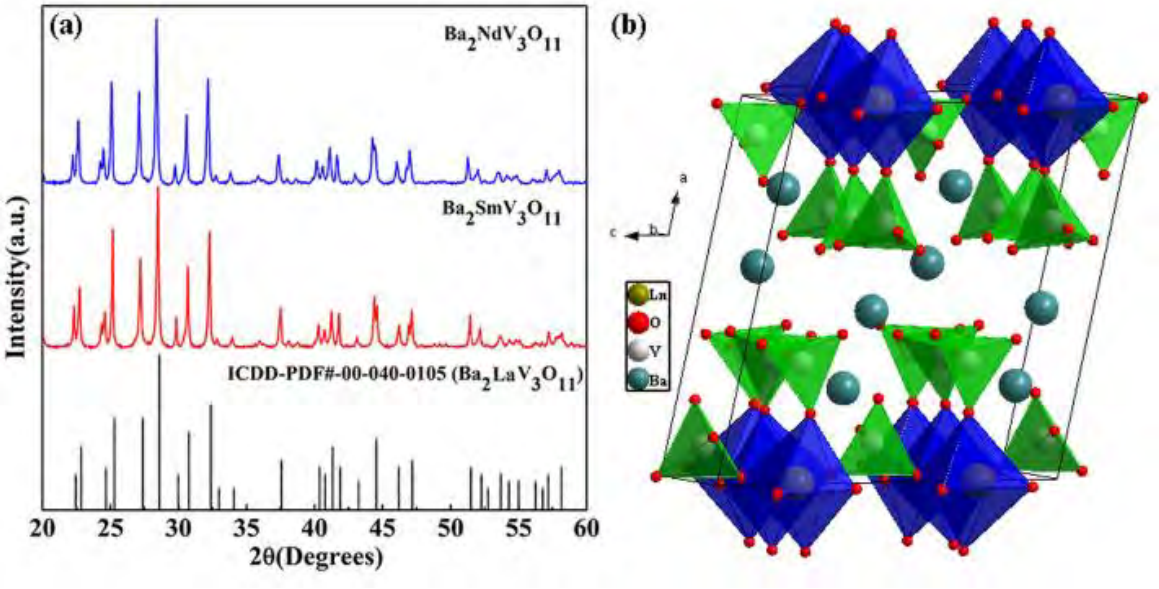
(a)
Ba$_2$NdV$_3$O$_{11}$
Ba$_2$SmV$_3$O$_{11}$
ICDD-PDF#-00-040-0105 (Ba$_2$LaV$_3$O$_{11}$)
Intensity(a.u.)
20
25
30
35
40
45
50
55
60
2θ(Degrees)
(b)
a
c
b
Ln
O
V
Ba

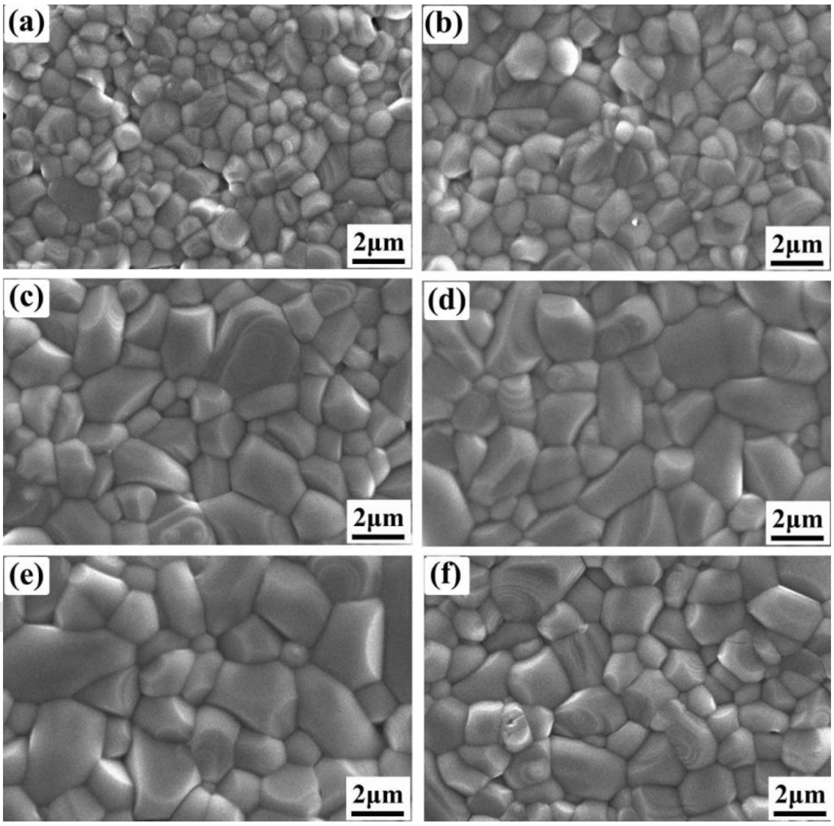
(a)
2μm
(b)
2μm
(c)
2μm
(d)
2μm
(e)
2μm
(f)
2μm

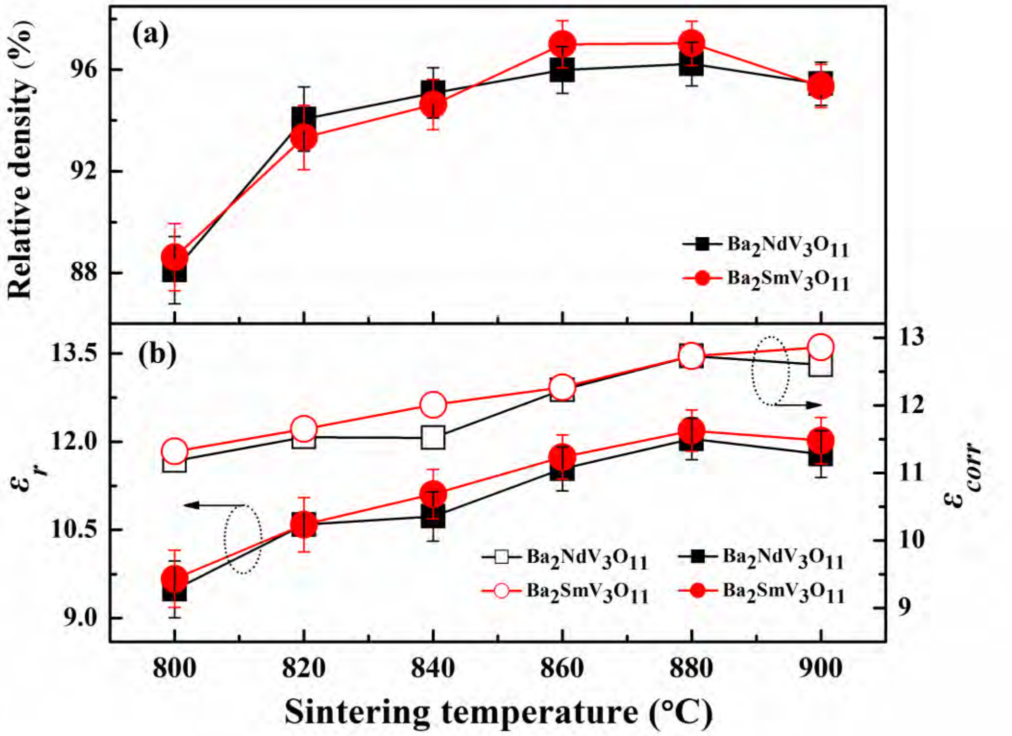
(a)
Relative density (%)
96
92
88
Ba2NdV3O11
Ba2SmV3O11
(b)
εr
13.5
12.0
10.5
9.0
εcorr
13
12
11
10
9
Ba2NdV3O11
Ba2NdV3O11
Ba2SmV3O11
Ba2SmV3O11
800
820
840
860
880
900
Sintering temperature (°C)

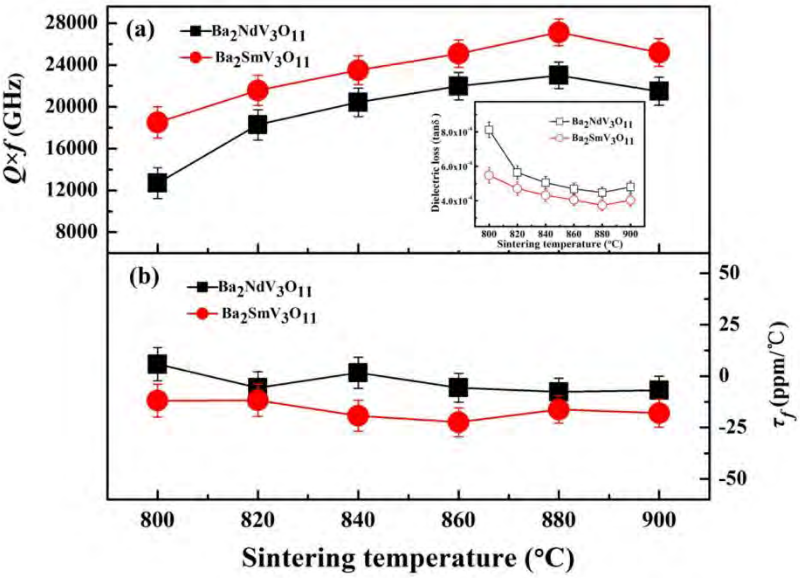
(a)
Ba2NdV3O11
Ba2SmV3O11
Q×f (GHz)
28000
24000
20000
16000
12000
8000
Dielectric loss (tanδ)
8.0x10-4
6.0x10-4
4.0x10-4
800 820 840 860 880 900
Sintering temperature (°C)
(b)
Ba2NdV3O11
Ba2SmV3O11
τf (ppm/℃)
50
25
0
-25
-50
800
820
840
860
880
900
Sintering temperature (°C)

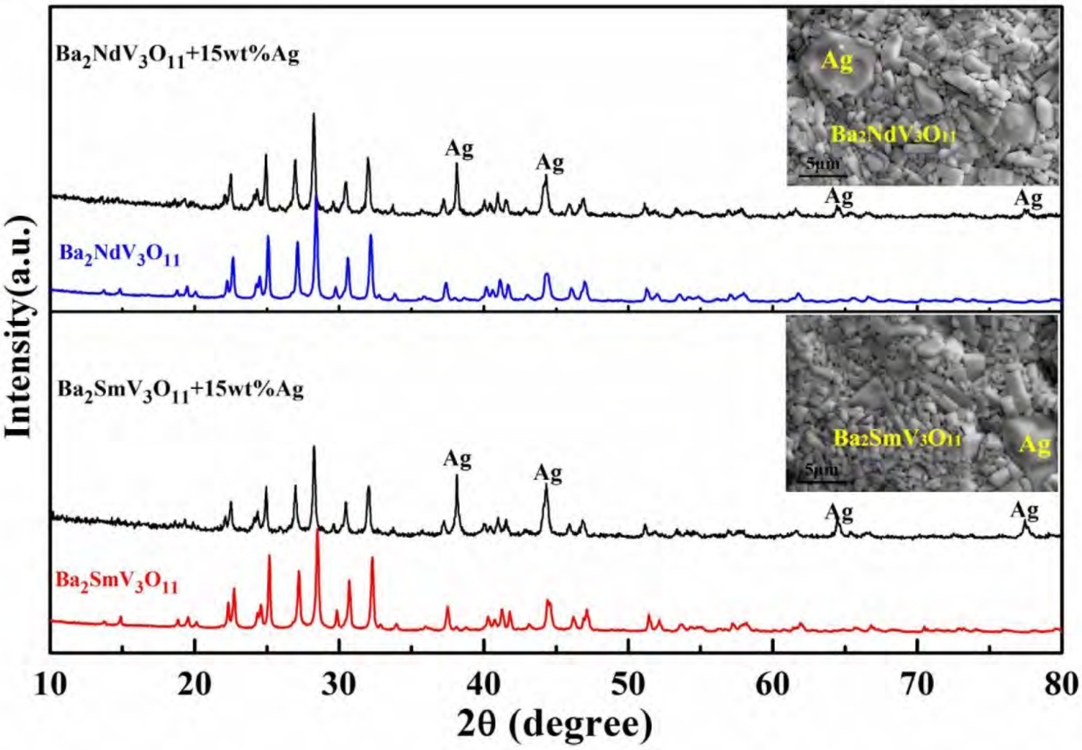
Ba2NdV3O11+15wt%Ag
Ag
Ag
Ag
Ag
Ag
Ba2NdV3O11
5μm
Ba2NdV3O11
Intensity(a.u.)
Ba2SmV3O11+15wt%Ag
Ba2SmV3O11
Ag
5μm
Ag
Ag
Ag
Ag
Ba2SmV3O11
10
20
30
40
50
60
70
80
2θ (degree)

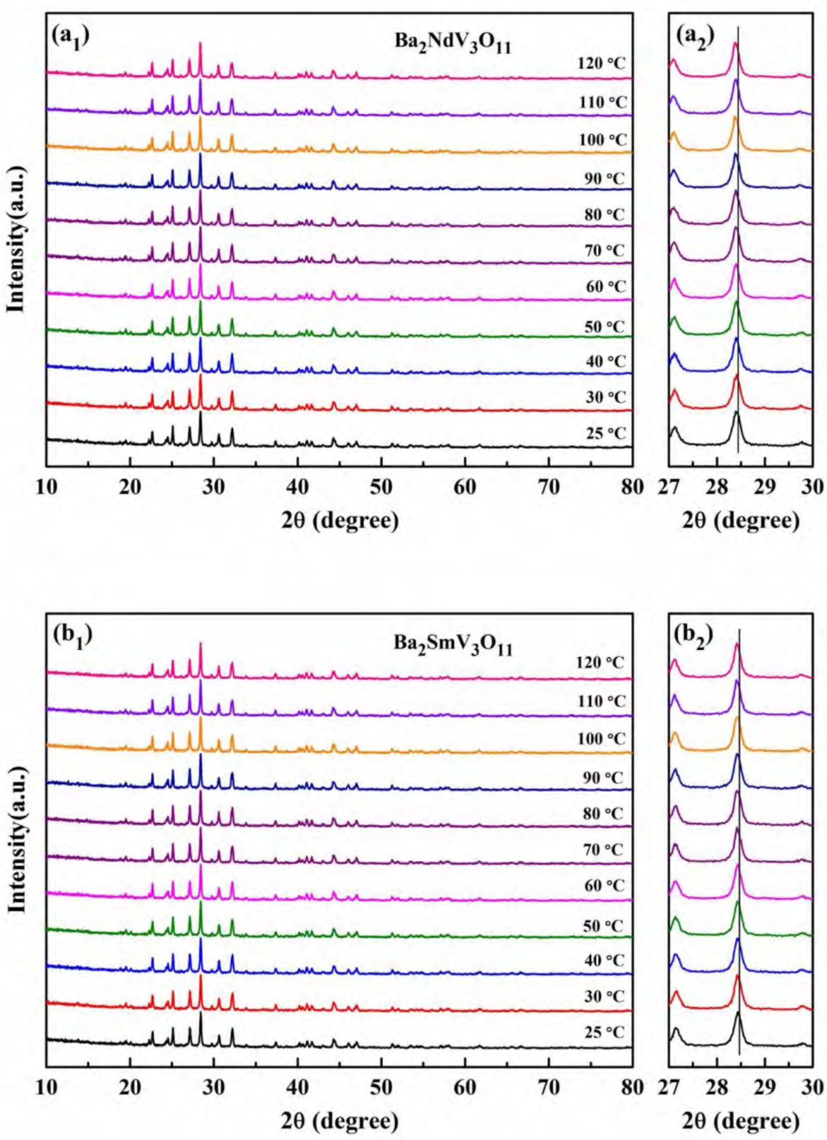
(a1)
Ba2NdV3O11
(a2)
(b1)
Ba2SmV3O11
(b2)
Intensity(a.u.)
120 °C
110 °C
100 °C
90 °C
80 °C
70 °C
60 °C
50 °C
40 °C
30 °C
25 °C
10
20
30
40
50
60
70
80
27
28
29
30
2θ (degree)

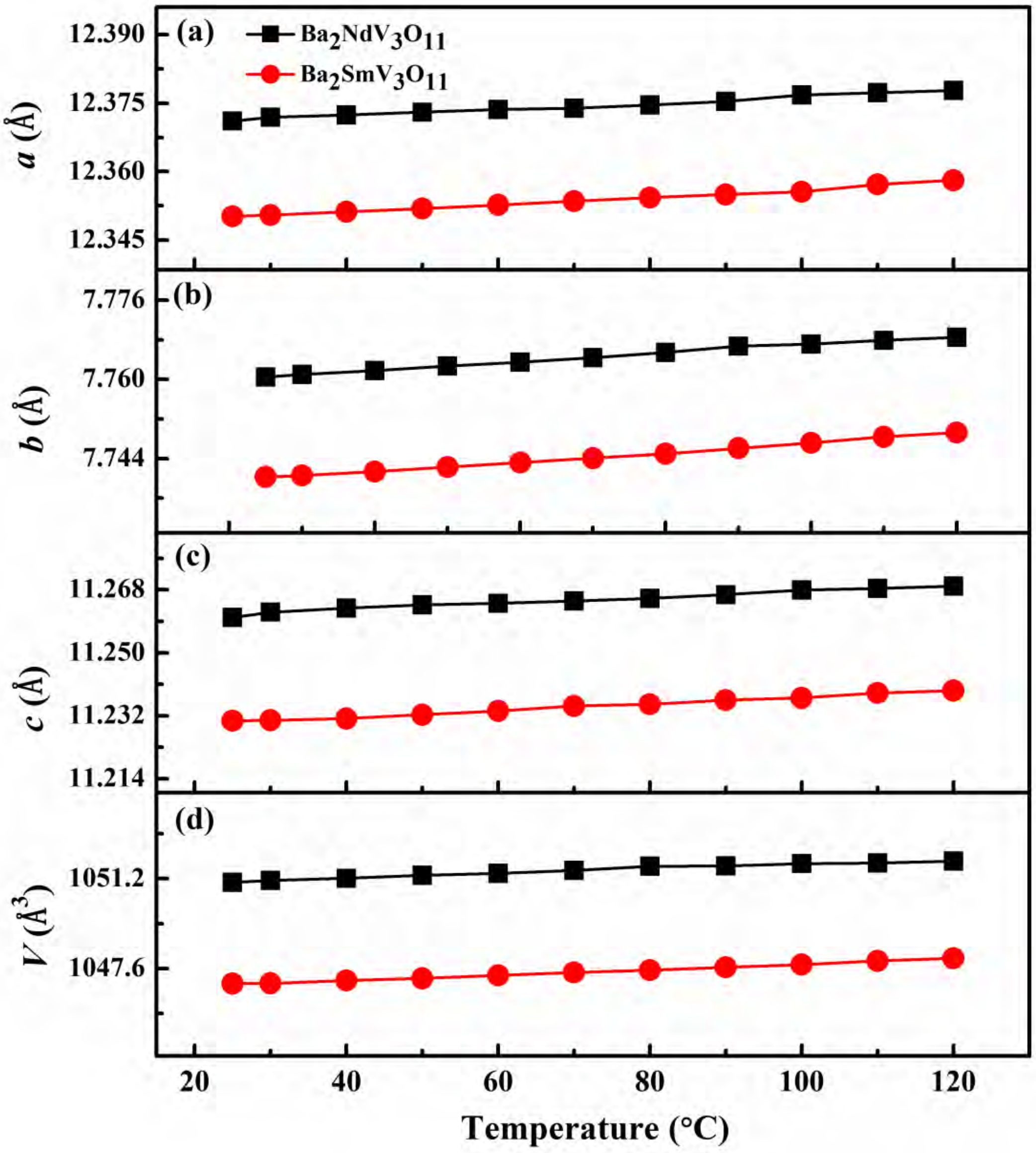
(a)
(b)
(c)
(d)
Ba$_2$NdV$_3$O$_{11}$
Ba$_2$SmV$_3$O$_{11}$
a (Å)
12.390
12.375
12.360
12.345
b (Å)
7.776
7.760
7.744
c (Å)
11.268
11.250
11.232
11.214
V (Å^3)
1051.2
1047.6
20
40
60
80
100
120
Temperature (°C)